11

Performance Analysis and Optimization of Sizable 6-axis Force Sensor Based on Stewart Platform

Y. Z. Zhao, T. S. Zhao, L. H. Liu, H. Bian and N. Li
Robotics Research Center, Yanshan University
P. R. China

1. Introduction

The Stewart platform, originally proposed for a flight simulator by Stewart (1965) has been suggested for a variety of applications by Hunt (1978), Fichter (1986) and Portman (2000). The advantage of the compact design with six degrees of freedom prompts one to consider the mechanism for force-torque sensor application. The parallel 6-axis force sensor is a kind of measure instrument which has the ability of detecting the forces and moments in x, y, and z directions simultaneously. The 6-axis force-torque sensor has been widely used in the situation of force/force-position control, such as parts teaching, contour tracking, precision assembly, etc. in addition to the applications in thrust testing of rocket engines and wind tunnel by Gaillet (1983) and Kaneko (1996).

Performance analysis and optimization design are important during the design of the sensor. There are a lot of literatures available on the design of force-torque sensor. Kerr (1989) analyzed an octahedral structure and enumerated a few design criteria for the sensor structure. Uchiyama and Hakomoic (1985) studied the isotropy of force sensor. Bicchi (1992) discussed the optimization of force sensor. Xiong (1996) defined the isotropy of force sensor on the basis of the information matrix. Jin (2003) presented the indices design method for 6-axis force sensor used on a dexterous hand. Ranganath (2004) studied the performances of the force sensor in the near-singular configuration. Tao (2004) optimized the performances of force sensor with finite element method. Theoretical and experimental investigations of the Stewart platform sensor were carried out by various authors, namely Romiti and Sorli (1992), Zhmud (1993) and Dai (1994) etc. So far, the researchers have obtained many achievements in the field of 6-axis force sensor, but the performances of the sizable parallel 6-axis force sensor prototype based on Stewart platform varies largely in different directions. The further application of the sizable parallel sensor is blocked by the existent performance anisotropy. So, the performance analysis and optimization design is significant to evaluating performances and the conceptual design of the sizable parallel sensor based on Stewart platform.

This paper presents the performance analysis and optimization design of the sizable parallel 6-axis force sensor with Stewart platform. The paper is organized as follows. Section 2

Source: Sensors, Focus on Tactile, Force and Stress Sensors, Book edited by: Jose Gerardo Rocha and Senentxu Lanceros-Mendez,
ISBN 978-953-7619-31-2, pp. 444, December 2008, I-Tech, Vienna, Austria

presents the static mathematics model of the 6-axis force sensor with screw theory. The static force influence coefficient matrix and the generalized force Jacobian matrix of the 6-axis force sensor are derived. Based on the screw theory and the theory of physical model of the solution space, some performances indices are defined. The force isotropy, torque isotropy, force sensitivity isotropy and torque sensitivity isotropy indices atlases of the 6-axis force sensor are plotted, and the rules how structure parameters affect the performances indices are summarized in Section 3. The optimization method of sizable parallel 6-axis force sensor's structure parameters is proposed, and an optimization numerical example is demonstrated in nonlinear single objective and multi-objective in section 4, respectively. Based on the result of the performances analysis and optimization, the section 5 presents a novel sizable 6-axis force sensor with flexible joints, which can avoid effectively the friction and the clearance in general spherical joint and has a wider application foreground. The research result reported of the chapter is concluded in section 6, future research in section 7, acknowledgement in section 8, and references in section 9.

2. Static mathematics model of 6-axis force sensor

The Stewart platform 6-axis force sensor is a kind of special parallel mechanism that is symmetrical design. Fig.1 is the sketch of the mechanism and forces acted on the platform. The platforms of the upper and lower platform are shown in Fig.2. O_u-$X_uY_uZ_u$ is the coordinate system fixed on the center point **P** of the upper platform, when the upper platform and the lower are both in the horizontal position. The spherical joints connecting links and upper platform at the upper ends are signed $a_i \ (i = 1, 2, \cdots, 6)$ while the spherical joints in the lower and the corresponding position vectors are $\boldsymbol{A}_i \ (i = 1, 2, \cdots, 6)$ and $\boldsymbol{B}_i \ (i = 1, 2, \cdots, 6)$ respectively. Each link will be subjected only to the axial force, ignoring the links' gravitation and the friction between joints.

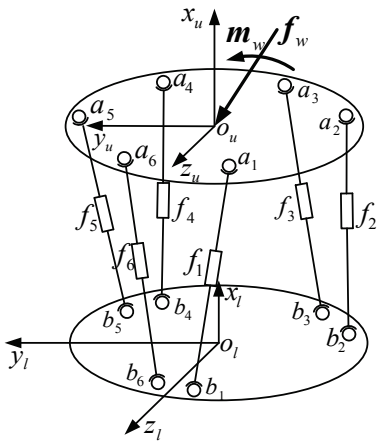

Fig. 1. The sketch of 6-axis force sensor based on Stewart platform

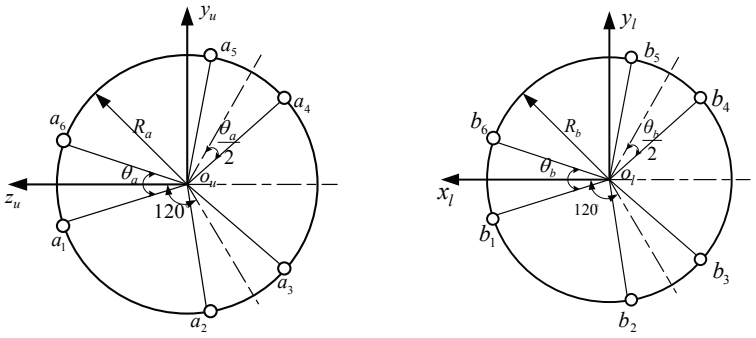

Fig. 2. The upper and lower platform of 6-axis force sensor's

Investigating the upper platform, the force equation based on the screw theory and static equilibrium can be obtained as

$$\boldsymbol{F}_w = \sum_{i=1}^{6} f_i \$_i \tag{1}$$

where, f_i is magnitude of the *i*th link's axial force, $\$_i = \left(\boldsymbol{S}_i ; \boldsymbol{S}_{0i}\right)^T$ expresses the unit vector of ith link's direction, and $\boldsymbol{F}_w = \left(\boldsymbol{f}_w \ \ \boldsymbol{m}_w\right)^T$ is the generalized external force applied to the upper platform. $\boldsymbol{f}_w = \left(f_{wx} \ \ f_{wy} \ \ f_{wz}\right)^T$ and $\boldsymbol{m}_w = \left(m_{wx} \ \ m_{wy} \ \ m_{wz}\right)^T$ are the external force and moment. The above equation can be disintegrated as

$$\begin{aligned} \boldsymbol{f}_w &= \sum_{i=1}^{6} f_i \boldsymbol{S}_i \\ \boldsymbol{m}_w &= \sum_{i=1}^{6} f_i \boldsymbol{S}_{0i} \end{aligned} \tag{2}$$

where, $\boldsymbol{S}_i = \left(\boldsymbol{a}_i - \boldsymbol{b}_i\right) \Big/ \left|\boldsymbol{a}_i - \boldsymbol{b}_i\right|$ and $\boldsymbol{S}_{0i} = \left(\boldsymbol{b}_i \times \boldsymbol{a}_i\right) \Big/ \left|\boldsymbol{a}_i - \boldsymbol{b}_i\right|$. So, the equation (1) can be also expressed as $\boldsymbol{F}_w = \boldsymbol{G}\,\boldsymbol{f}$, where $\boldsymbol{f} = \left(f_1 \ f_2 \ f_3 \ f_4 \ f_5 \ f_6\right)^T$. The static force influence coefficient matrix of the parallel 6-axis force sensor can be expressed as

$$\boldsymbol{G} = \begin{bmatrix} \boldsymbol{S}_1 & \boldsymbol{S}_2 & \cdots & \boldsymbol{S}_6 \\ \boldsymbol{S}_{01} & \boldsymbol{S}_{02} & \cdots & \boldsymbol{S}_{06} \end{bmatrix} \tag{3}$$

The former three rows of the matrix $\boldsymbol{G}$ is the force transmitting factor of the parallel sensor, while the latter three rows is the torque-transmitting factor. The factors having different unit, which the former is dimensionless, while the latter has length unit, the matrix $\boldsymbol{G}$ is disintegrated into the static force influence coefficient matrix $\boldsymbol{G}_1$ and the static torque influence coefficient matrix $\boldsymbol{G}_2$. That is $\boldsymbol{G} = \left[\boldsymbol{G}_1 \ \ \boldsymbol{G}_2\right]^T$. The transformational relation between the generalized external force in 6 dimensions and the link's axial force can be given as

$$\boldsymbol{J}\,\boldsymbol{F}_w = \boldsymbol{f} \tag{4}$$

where, $\boldsymbol{J} = \boldsymbol{G}^{-1}$ is the generalized force Jacobian matrix of the parallel 6-axis sensor. Similarly, the generalized force Jacobian matrix $\boldsymbol{J}$ is disintegrated into the force Jacobian matrix $\boldsymbol{J}_1$ and the torque Jacobian matrix $\boldsymbol{J}_2$, that is $\boldsymbol{J} = \begin{bmatrix} \boldsymbol{J}_1 & \boldsymbol{J}_2 \end{bmatrix}$.

3. Performance analysis of parallel 6-axis force sensor

3.1 Physical model of the solution space theory

The physical model of the solution space theory has the ability to show all possible size combination of the mechanism. It is convenient to obtain the law of the sensor's indices following the changing of the element structure parameters. From the static mathematics model of the force sensor above, the 6-axis force sensor based on Stewart platform contains four structure parameters. That is the radius R_a of the upper platform, the radius R_b of the lower platform, the height H between platforms, and the angle difference $\theta_{ab} = \theta_a - \theta_b$ between the corresponding twin link of the upper and the lower platform. With the precondition of θ_{ab} is changeless, let $R_a + R_b + H = T$, then

$$\frac{R_a}{T} + \frac{R_b}{T} + \frac{H}{T} = 1 \tag{5}$$

Let $r_a = \dfrac{R_a}{T}$, $r_b = \dfrac{R_b}{T}$ and $r_c = \dfrac{R_c}{T}$, the equation (5) gives

$$r_a + r_b + r_H = 1 \tag{6}$$

where, $0 < r_a < 1$, $0 < r_b < 1$, $0 < r_H < 1$. Thus, the physical model of the solution space theory of the 6-axis force sensor based on Stewart platform is developed. For displaying conveniently, the physical model can be transformed into two dimension *O-XY* plane as shown in Fig. 3. The transformation between the coordinates can be expressed as

$$x = \frac{2\sqrt{3}}{3} \cdot r_b + \frac{\sqrt{3}}{3} \cdot r_H \text{ and } y = r_H \tag{7}$$

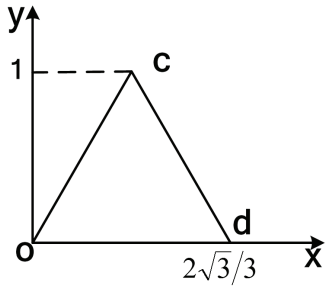

Fig. 3. The ichnography of the sensor's spacial model

Therefore, all possible parameters combination of the 6-axis force sensor based on Stewart platform are included in the triangle *ocd*. In other words, each point in the triangle ocd corresponds with a set of structure parameters. With the physical model of the solution space theory, selecting parameters and optimization structure design are convenient greatly.

3.2 Performances atlases analysis

The indices evaluating the performances of the 6-axis force sensor are the foundation of the performance evaluating and the optimization design. As for the parallel 6-axis force sensor, it should have high force isotropy, torque isotropy, and force/torque (F/T) sensitivity isotropy, in addition to the high sensitivity, precision, signal noise ratio (SNR) and speedy response. The performances atlases are plotted in the area of the physical model triangle ocd, based on the static mathematics model above and the defining of the performances indices given by Uchiyama and Hakomori (1985), Xiong (1996) and Jin (2003) with the force isotropy $u_1 = 1/\mathrm{cond}(\boldsymbol{G}_1)$, the torque isotropy $u_2 = 1/\mathrm{cond}(\boldsymbol{G}_2)$, the force sensitivity isotropy $u_3 = 1/\mathrm{cond}(\boldsymbol{J}_1)$ and the torque sensitivity isotropy $u_4 = 1/\mathrm{cond}(\boldsymbol{J}_2)$. From the sensor's physical model of the solution space theory developed above, the performances atlases varies with the angle θ_{ab}. It is unpractical to show all existent performances atlases. Considering the latter optimization design of the structure parameters, the performances spacial and planar atlases are plotted as shown in Fig. 4-11, respectively, when the coordinate system fixed on the center point of the lower platform and $\theta_{ab} = 60^\circ$. It can be easily gotten the indices distributing laws with the performances atlases of force isotropy, torque isotropy, force sensitivity isotropy and torque sensitivity isotropy, especially in the planar atlases of as shown in Fig.5, Fig.7, Fig.9 and Fig.11.

From the influence that the structure parameters act on the sensor's performances indices shown in Fig. 4-11, the laws guiding the optimization design can be concluded as following. The plot of the force isotropy distributes parabola approximately in the area of the physical model as shown in Fig. 4 and Fig. 5. The force isotropy will becomes higher in the middle and lower area of the physical model. The corresponding structure parameters can be selected, when the index of the force isotropy should be attached importance to design.

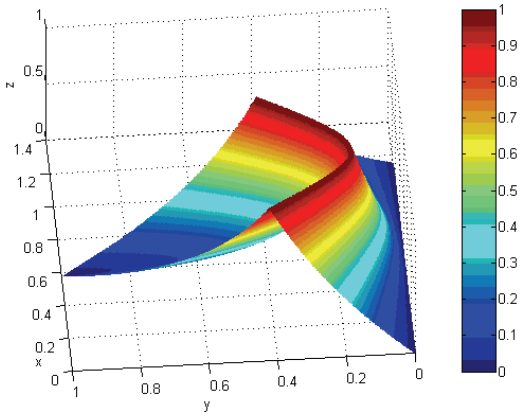

Fig. 4. Force isotropy spacial atlas with respect to $\theta_{ab} = 60^\circ$

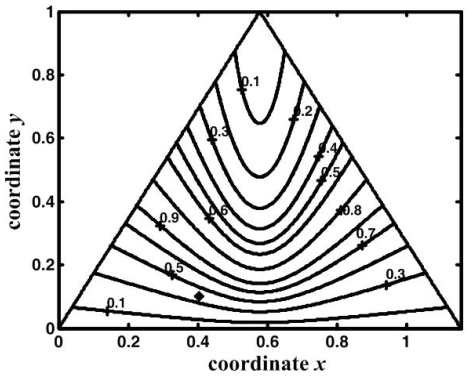

Fig. 5. Force isotropy planar atlas with respect to $\theta_{ab} = 60^{\circ}$

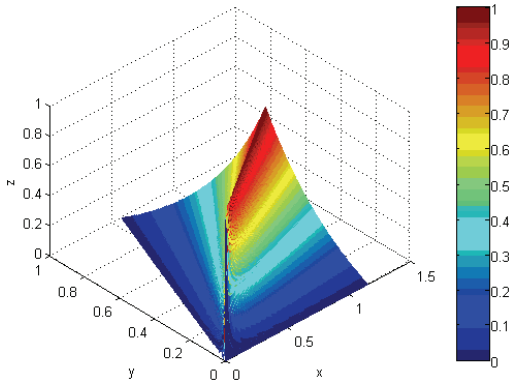

Fig. 6. Torque isotropy spacial atlas with respect to $\theta_{ab} = 60^{\circ}$

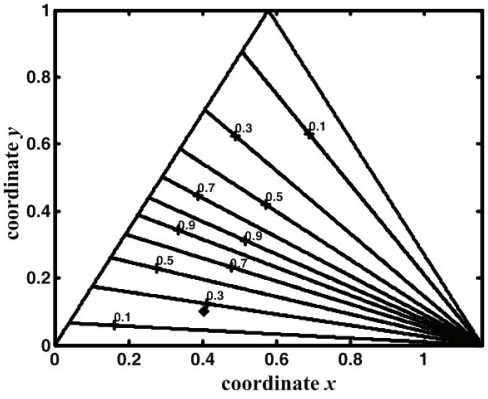

Fig. 7. Torque isotropy planar atlas with respect to $\theta_{ab} = 60^{\circ}$

The plot of the torque isotropy distributes beeline approximately in the area of the physical model as shown in Fig. 6 and Fig. 7. The torque isotropy will becomes lower in the right side and upper area of the physical model. The corresponding structure parameters should be eliminated, when the index of the torque isotropy should be attached importance to design.

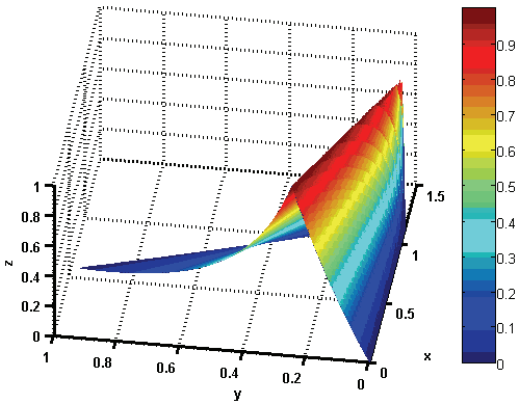

Fig. 8. Force sensitivity isotropy spatial atlas with respect to $\theta_{ab} = 60^{\circ}$

The plot of the force sensitivity isotropy distributes beeline approximately in the area of the physical model as shown in Fig. 8 and Fig.9. The force sensitivity isotropy will change rapidly by the x axis in the physical model. The corresponding structure parameters should be eliminated in design. In the upper most area, the index of the force sensitivity isotropy is smaller. The force sensitivity isotropy distributing resembles the torque isotropy distributing of the force sensor.

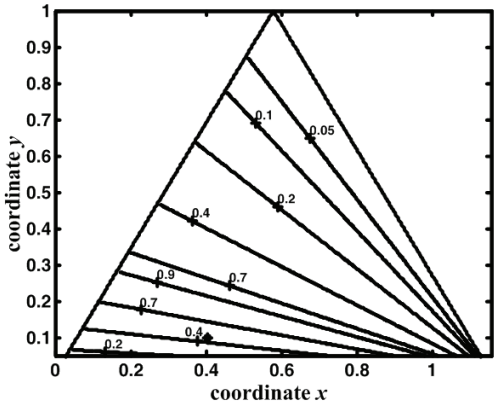

Fig. 9. Force sensitivity isotropy planar atlas with respect to $\theta_{ab} = 60^{\circ}$

The plot of the torque sensitivity isotropy distributes parabola approximately in the area of the physical model as shown in Fig. 10 and Fig. 11. The torque sensitivity isotropy will becomes higher in the middle part of the physical model. The corresponding structure parameters can be selected, when the index should be attached importance to design.

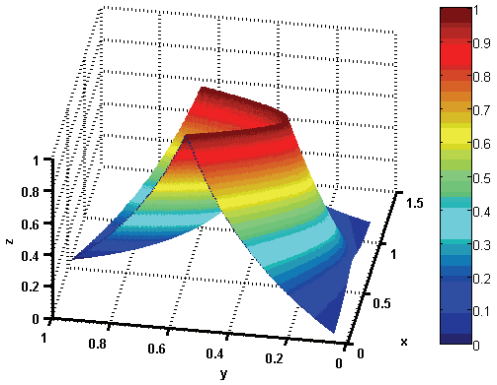

Fig. 10. Torque sensitivity spacial isotropy atlas with respect to $\theta_{ab} = 60^{\circ}$

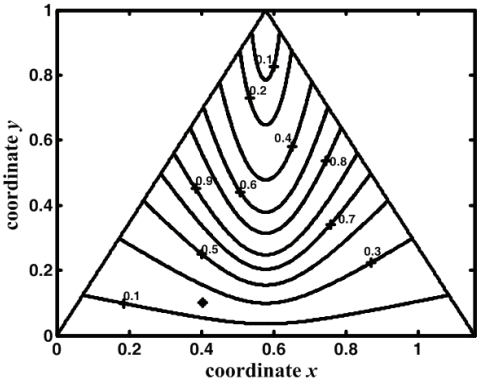

Fig. 11. Torque sensitivity planar isotropy atlas with respect to $\theta_{ab} = 60^{\circ}$

4. Optimization design of sizable parallel 6-axis force sensor

4.1 Optimization objective function

In the sensor's practical application, the request for the performances indices varies with the practical application cases. Some performance index should be considered principally in some cases, while the comprehensive performance index is pivotal in some cases. The paper optimizes the existing sensor's structure parameters in nonlinear single objective and multi-objective respectively, in order to obtain better performances than that of the initial ones. As the restriction of mechanical special model, the constraint equation $0 \le |\theta_{ab}| \le 120°$ should be applied. In the single objective optimum, the objective functions are chosen as following

$$f_{FD}(R_a \quad R_b \quad H \quad \theta_{ab}) = [\lambda_{\max}(\boldsymbol{G}_1^{\boldsymbol{T}} \cdot \boldsymbol{G}_1)]^{1/2} / [\lambda_{\min}(\boldsymbol{G}_1^{\boldsymbol{T}} \cdot \boldsymbol{G}_1)]^{1/2} \tag{8}$$

$$f_{MD}(R_a \quad R_b \quad H \quad \theta_{ab}) = [\lambda_{\max}(\boldsymbol{G}_2^{\boldsymbol{T}} \cdot \boldsymbol{G}_2)]^{1/2} / [\lambda_{\min}(\boldsymbol{G}_2^{\boldsymbol{T}} \cdot \boldsymbol{G}_2)]^{1/2} \tag{9}$$

$$f_{FS}\left(R_a \;\; R_b \;\; H \;\; \theta_{ab}\right) = [\lambda_{\max}(\boldsymbol{J}_1^T \cdot \boldsymbol{J}_1)]^{1/2} \Big/ [\lambda_{\min}(\boldsymbol{J}_1^T \cdot \boldsymbol{J}_1)]^{1/2} \tag{10}$$

$$f_{MS}\left(R_a \;\; R_b \;\; H \;\; \theta_{ab}\right) = [\lambda_{\max}(\boldsymbol{J}_2^T \cdot \boldsymbol{J}_2)]^{1/2} \Big/ [\lambda_{\min}(\boldsymbol{J}_2^T \cdot \boldsymbol{J}_2)]^{1/2} \tag{11}$$

The objective functions in the above equation (8)-(11) are the reciprocals of the force isotropy u_1, the torque isotropy u_2, the force sensitivity isotropy u_3 and the torque sensitivity isotropy u_4, respectively. When the objective function reaches the minimum, the corresponding performance index attains the maximum. When the comprehensive performance is pivotal, the multi-objective optimum would be executed to obtain the sensor with the high performances. The corresponding objective function can be expressed as

$$f_G\left(R_a \;\; R_b \;\; H \;\; \theta_{ab}\right) = \min\left(k_{FD} \cdot f_{FD} + k_{MD} \cdot f_{MD} + k_{FS} \cdot f_{FS} + k_{MS} \cdot f_{MS}\right) \tag{12}$$

where, k_{FD}, k_{MD}, k_{FS}, and k_{MS} are the weights of the corresponding indices. During the practical optimization, the weight matrix $\boldsymbol{k} = \left[k_{FD}\; k_{MD}\; k_{FS}\; k_{MS}\right]$ can be set as the weights of the corresponding performances indices.

4.2 Optimization numerical examples

Considering the practical structure parameters of the sizable parallel 6-axis force sensor, the initial parameters are set as $R_a = 720$ mm, $R_b = 360$ mm, $H = 120$ mm, $\theta_{ab} = 60^\circ$. With the Matlab optimization toolbox and the defined objective functions, the corresponding optimal design parameters are obtained. Based on the force isotropy single objective optimization, the optimal parameters can be obtained as $R_a = 692$ mm, $R_b = 378$ mm, $H = 228$ mm and $\theta_{ab} = 17^\circ$. The force isotropy of the sensor with the optimal parameters $u_1 = 1.0000$ with respect to the initial $u_1 = 0.3804$. Based on the torque isotropy single objective optimization, the optimal parameters can be obtained as $R_a = 715$ mm, $R_b = 360$ mm, $H = 144$ mm and $\theta_{ab} = 16^\circ$. The torque isotropy u_2 of the sensor with the optimal parameters improves to 1.0000 from the initial $u_1 = 0.2357$. When the force sensitivity isotropy is optimized, the optimal parameters can be obtained as $R_a = 713$ mm, $R_b = 373$ mm, $H = 95$ mm and $\theta_{ab} = 60^\circ$. Whereafter, the force sensitivity isotropy u_3 improves to 1.0000 from the initial 0.4714. When the torque sensitivity isotropy is optimized, the optimal parameters can be obtained as $R_a = 634$ mm, $R_b = 424$ mm, $H = 357$ mm and $\theta_{ab} = 31^\circ$. Whereafter, the torque sensitivity isotropy u_4 improves to 1.0000 from the initial 0.2116.

In the multi-objective optimization, the comprehensive performances indices should be taken into account synthetically. With the weight matrix ***k***=[1111], the optimal performance indices with respect to the comprehensive parameters and the corresponding initial indices are shown in Table 1. It is obvious that the performances of the sizable parallel 6-axis force sensor are improved. The corresponding performance indices of the initial structure parameters in Table 1 are shown in the planar atlas Fig. 5, Fig. 7, Fig. 9, and Fig. 11 with the "∗" symbol.

	R_a	R_b	H	θ_{ab}	u_1	u_2	u_3	u_4
Initial	720	360	120	60°	0.380	0.235	0.471	0.190
Optimal	614	450	418	85°	0.701	0.712	0.701	0.712

Table 1. Contrast multi-objective optimal result with the initial design

5. A novel sizable 6-axis force sensor with flexible joints

Based on the above analysis, optimization design and considering the machining technics synchronously, we design the a novel sizable 6-axis force sensor structure with flexible joints as shown in Fig. 12. Each branch is composed of UUR flexible joints and a standard pull and press force sensor. The axe of the flexible R joints go through the near U flexible joint, which can be considered as a sphere joint. The flexible joints here are the novel flexible joints which can carry the biggish loading. The six branches are divided the same 3 groups. The first U joints of the branches in some group are made in a whole material, similary as the last R joints of the branches in some group. Another design project with the same 6 unitary branch is shown as in Fig. 13.

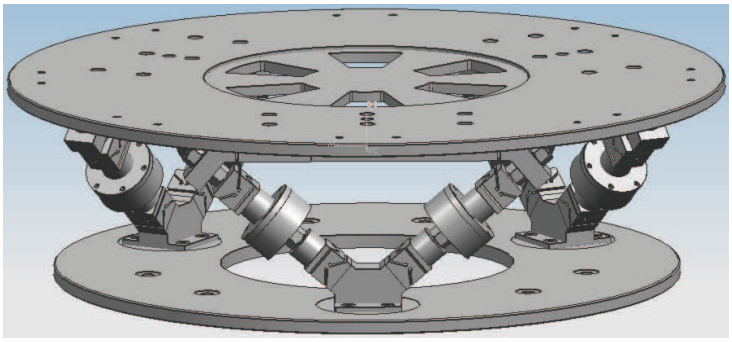

Fig. 12. A novel sizable 6-axis force sensor prototype with flexible joints

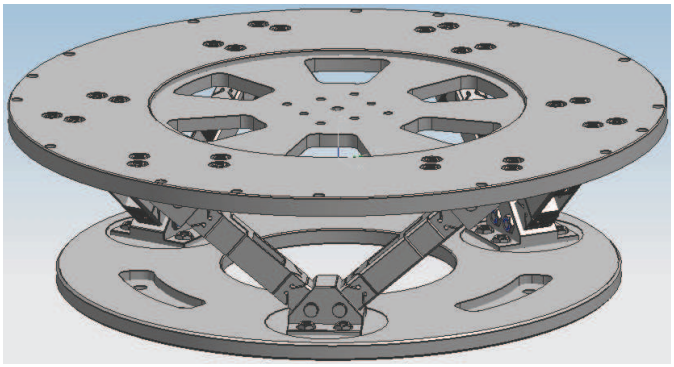

Fig. 13. Another sizable 6-axis force sensor prototype with flexible joints

6. Future research

The performance indices of the 6-axis force sensor based on Stewart platform shouled be further analyzed, especially dynamic performance index. The novel sizable 6-axis force sensor with flexible joints should be futher optimized, especially the stucture parameters of the flexible joints. The manufacture and calibration of the sizable 6-axis force sensor with flexible joints are also the future research.

7. Conclusion

The paper plots the indices atlases based on the screw theory and definition of the performances indices, and summaries the law how structure parameters affect the indices. With the constructed optimization objective functions, the sizable parallel 6-axis force sensor's structure parameters are optimized in nonlinear single objective and multi-objective respectively. The corresponding optimal structure parameters are obtained. A novel sizable 6-axis force sensor with flexible joints is developped. So, the powerful basis and method are raised for design and optimization of sizable parallel 6-axis force sensor based on Stewart platform.

8. Acknowledgment

The research work reported here is supported by National Natural Science Foundation of China (NSFC) under Grant No.50375134 and No.50675191.

9. References

Stewart D. (1965). A Platform with Six Degrees of Freedom. *Proc. Inst. Mech.*, Part 1 180 (15), 371-386.

Hunt K. H. (1978). *Kinematic Geometry of Mechanisms*, Clarendon Press, Oxford.

Fichter E. F. (1986). The Stewart Platform Manipulator: General Theory and Practical Construction. *Int. J. Robot. Res*, 5(2), 157-182.

Portman V. T.; Sandler B. & Zahavi E. (2000). Rigid 6×6 Parallel Platform for Precision 3-D Micro-manipulation: Theory and Design Application. *IEEE Trans. Robot. Automat*, 16(6), 629-643.

Gaillet A. & Reboulet C. (1983). An Isostatic Six Component Force and Torque Sensor. *Proc. 13th Int. Symposium on Industrial Robotics*, pp. 783-792.

Kaneko M. (1996). Twin-head Six-axis Force Sensor. *IEEE Trans. Robot. Automat*, 12(1), 146-154.

Kerr D. R. (1989), Analysis, Properties and Design of Stewart Platform Transducer. *Trans. ASME. J. Mech. Transm. Automn*, 111, pp. 25-28.

Uchiyama M. & Hakomori K.A. (1985). Few Considerations on Structure Design of Force Sensors. *Proceedings of the Third Annual Conf. Japan Robotics Society*, pp. 17-18.

Bicchi A. (1992). A Criterion for Optimal Design of Multi-axis Force Sensors. *Robotics and Autonomous Systems*, 10(4), 269-286.

Xiong Y. L. (1996). On Isotropy of Robot's Force Sensors. *Acta Automatica Sinica*, 22(1), 10-18. (in Chinese)

Jin Z. L.; Zhao X. C. & Gao F. (2003). The Research on Link Length Design of a Novel Dexterous Hand's 6-axis Force Transducer. *Chinese Journal of Scientific Instrument*, 24(4), 371-374.

R. Ranganath, et al (2004). A Force-torque Sensor Based on a Stewart Platform in a Near-Singular Configuration. *Mechanism and Machine Theory*, 39, pp. 971-998.

Tao L.; Yoshi I. & Kyoko S. (2004). A Six-dimension Parallel Force Sensor for Human Dynamics Analysis. *Proceedings of the IEEE Conference on Robotics, Automation and Mechatronics*, pp. 208-212.

Romiti A. & Sorli M. (1992). Force and Moment Measurement on a Robotic Assembly Hand. *Sensors Actuators A*, 32, pp. 531-538.

Sorli M. & Zhmud N. (1993). Investigation of Force and Moment Measurement System for a Rotating Assembly Hand. *Sensors Actuators A*, 37, pp. 651-657.

Dai J. S.; C. Sodhi & Kerr D. R. (1994). Design and Analysis of a New Six-component Force Transducer for Robotic Grasping. *Proceeding of the Second Biennial European Joint Conference on Engineering Systems Design and Analysis*, ASME PD, pp. 809-817.

Sensors: Focus on Tactile Force and Stress Sensors

Edited by Jose Gerardo Rocha and Senentxu Lanceros-Mendez

ISBN 978-953-7619-31-2
Hard cover, 444 pages
Publisher InTech
Published online 01, December, 2008
Published in print edition December, 2008

This book describes some devices that are commonly identified as tactile or force sensors. This is achieved with different degrees of detail, in a unique and actual resource, through the description of different approaches to this type of sensors. Understanding the design and the working principles of the sensors described here requires a multidisciplinary background of electrical engineering, mechanical engineering, physics, biology, etc. An attempt has been made to place side by side the most pertinent information in order to reach a more productive reading not only for professionals dedicated to the design of tactile sensors, but also for all other sensor users, as for example, in the field of robotics. The latest technologies presented in this book are more focused on information readout and processing: as new materials, micro and sub-micro sensors are available, wireless transmission and processing of the sensorial information, as well as some innovative methodologies for obtaining and interpreting tactile information are also strongly evolving.

How to reference

In order to correctly reference this scholarly work, feel free to copy and paste the following:

Y. Z. Zhao, T. S. Zhao, L. H. Liu, H. Bian and N. Li (2008). Performance Analysis and Optimization of Sizable 6-Axis Force Sensor Based on Stewart Platform, Sensors: Focus on Tactile Force and Stress Sensors, Jose Gerardo Rocha and Senentxu Lanceros-Mendez (Ed.), ISBN: 978-953-7619-31-2, InTech, Available from: http://www.intechopen.com/books/sensors-focus-on-tactile-force-and-stress-sensors/performance_analysis_and_optimization_of_sizable_6-axis_force_sensor_based_on_stewart_platform

INTECH
open science | open minds

InTech Europe
University Campus STeP Ri
Slavka Krautzeka 83/A
51000 Rijeka, Croatia
Phone: +385 (51) 770 447
Fax: +385 (51) 686 166
www.intechopen.com

InTech China
Unit 405, Office Block, Hotel Equatorial Shanghai
No.65, Yan An Road (West), Shanghai, 200040, China
中国上海市延安西路65号上海国际贵都大饭店办公楼405单元
Phone: +86-21-62489820
Fax: +86-21-62489821